The continuum limit of 2+1 flavor DWF ensembles

Christopher Kelly[*]

Columbia University,
905 Pupin Hall,
116th St & Broadway,
New York, NY 10027, USA.
E-mail: ckelly@phys.columbia.edu

Peter Boyle

School of Physics,
The University of Edinburgh,
James Clerk Maxwell Building, King's Buildings,
Mayfield Road,
Edinburgh EH9 3JZ, UK.
E-mail: paboyle@ph.ed.ac.uk

For the RBC and UKQCD collaborations

We present light pseudoscalar physics in the continuum limit of 2+1 flavour domain wall QCD by the RBC and UKQCD. We make use of a fermion action with good chiral symmetry and use two different lattice spacings.

We use a new approach to match ensembles within the range of simulated masses, and apply a simultaneous chiral and continuum extrapolation. We discuss the evidence for chiral curvature in our data and present continuum results for pion and kaon decay constants, f_K/f_π, quark masses and the neutral kaon mixing parameter B_K.

The XXVIII International Symposium on Lattice Field Theory
June 14-19,2010
Villasimius, Sardinia Italy

[*]Speaker.

1. Introduction

In these proceedings we present continuum results for several light hadronic quantities obtained through a combined chiral and continuum extrapolation of the RBC and UKQCD collaboration's $32^3 \times 64$ and $24^3 \times 64$ domain wall fermion ensemble sets with $L_s = 16$ and the Iwasaki gauge action at $\beta = 2.25$ and 2.13 respectively. These are henceforth referred to as the 32^3 and 24^3 ensemble sets respectively. The lattice spacings, as determined by the combined analysis, are $2.28(3)$ GeV and $1.73(3)$ GeV such that the lightest unitary pion masses are ~ 290 MeV and ~ 330 MeV.

We discuss the definition of the scaling trajectory along which we take the continuum limit and give a brief account of the techniques used to fit and extrapolate our data. We then discuss the evidence for chiral curvature in our data and our strategy for estimating the systematic error associated with the chiral extrapolation. Finally we present results for the pion and kaon decay constants, quark masses and the neutral kaon mixing parameter B_K. Here the quark masses and B_K are renormalised into the $\overline{\text{MS}}$ scheme via several non-perturbative lattice momentum schemes with non-exceptional kinematics.

2. Fixing the scaling trajectory

In order to take the continuum limit we must define a *scaling trajectory*, that is the curve of $a\tilde{m}_s(\beta)$ and $a\tilde{m}_l(\beta)$ (for a 2+1f simulation) that is followed as $\beta \to \infty$. Here $a\tilde{m} = a(m + m_{\text{res}})$ is the DWF PCAC quark mass in lattice units. One method of defining the scaling trajectory is to choose values for two dimensionless physical quantities, labelled $\mathcal{R}_h$ and $\mathcal{R}_l$, and then to tune $a\tilde{m}_s(\beta)$ and $a\tilde{m}_l(\beta)$ such that these quantities remain constant as β is changed. In the continuum limit, all choices for the two dimensionless quantities are equivalent, whereas at finite β, the different choices for $\mathcal{R}_l$ and $\mathcal{R}_h$ result in $\mathcal{O}(a^2)$ differences between the values of other lattice quantities on the scaling curve. We choose $\mathcal{R}_l = (am_{ll})/(am_{hhh})$ and $\mathcal{R}_h = (am_{lh})/(am_{hhh})$, where am_{ll}, am_{lh} and am_{hhh} are the dimensionless pion, kaon and Ω-baryon masses at general (unitary) light and heavy quark masses.

In order to match to the real world, $\mathcal{R}_h$ and $\mathcal{R}_l$ should be fixed to their physical values in the continuum limit. Unfortunately this requires a sizeable extrapolation in the unitary light quark mass below the range of our data. In order to maximise statistics, this extrapolation is achieved through a combined fit to both the 32^3 and 24^3 ensemble sets, where the fit forms include explicit $\mathcal{O}(a^2)$ dependence. The chiral ansätze and the resulting fit forms are discussed in the next section.

Before we introduce the additional complexities of the chiral/continuum fit, it is useful to consider tuning to an *unphysical* scaling curve that passes through our data. We choose the values of $\mathcal{R}_l$ and $\mathcal{R}_h$ from the the 32^3 data at $am_l(32^3) = 0.006$ and $am_h(32^3) = 0.03$. The 24^3 data is then linearly interpolated to find the values of $am_l(24^3)$ and $am_h(24^3)$ at which those ratios match. This procedure is described in more detail in refs. [1] and [2]. We find the match point values $am_l(24^3) = 0.0058(1)$ and $am_h(24^3) = 0.0384(5)$. We can determine the ratio of lattice scales $R_a \equiv a(32^3)/a(24^3)$ from the ratio of a lattice quantity between the two lattices at the match point. Using the Ω-baryon mass, we find $R_a = m_{hhh}(32^3)/m_{hhh}(24^3) = 0.758(5)$. We also define two further quantities, Z_l and Z_h, from the ratios of light and heavy quark masses (in physical units) between the lattices;

$$Z_l = \frac{1}{R_a} \frac{a\tilde{m}_l(32^3)}{a\tilde{m}_l(24^3)} \text{ and } Z_h = \frac{1}{R_a} \frac{a\tilde{m}_h(32^3)}{a\tilde{m}_h(24^3)}, \tag{2.1}$$

for which we obtain $Z_l = 0.981(9)$ and $Z_h = 0.974(7)$.

Repeating this analysis using values of $\mathcal{R}_l$ and $\mathcal{R}_h$ obtained from several other data points on both lattices, we able to study the dependence of R_a, Z_l and Z_h upon the values of $\mathcal{R}_l$ and $\mathcal{R}_h$.
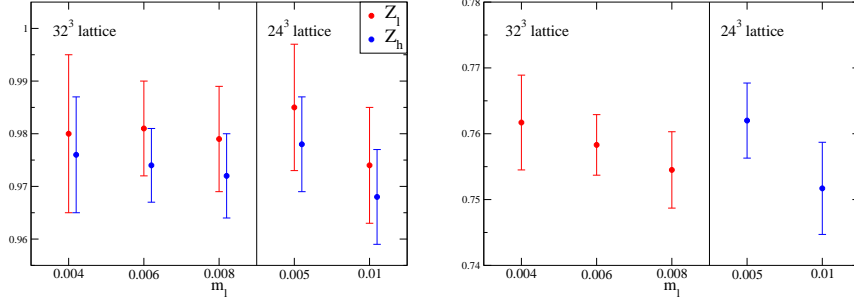
Figure 1: Z_l, Z_h (left) and R_a (right) obtained by matching at several different values of $\mathcal{R}_l$ and $\mathcal{R}_h$ obtained from the simulated data. The x-axis labels give the corresponding light quark mass. The heavy quark mass is fixed to $am_h(32) = 0.03$ and $am_h(24^3) = 0.04$ for match points on the 32^3 and 24^3 ensemble sets respectively.

The results of these analyses are shown in figure 1. We find no statistically significant dependence of these ratios upon the values of $\mathcal{R}_l$ and $\mathcal{R}_h$. This can be explained by considering two nearby scaling trajectories defined by $(\mathcal{R}_l, \mathcal{R}_h)$ and $(\mathcal{R}'_l, \mathcal{R}'_h)$ respectively, where the corresponding quark masses on the lattice e are $(a\tilde{m}^e_l, a\tilde{m}^e_h)$ and $(a\tilde{m}'^e_l, a\tilde{m}'^e_l)$. Expanding about the continuum limit,

$$\left(\frac{\tilde{m}'^e_l}{\tilde{m}^e_l} \right) = \lim_{\beta \to 0} \left(\frac{\tilde{m}'_l(\beta)}{\tilde{m}_l(\beta)} \right) + d_l (\Lambda_{\mathrm{QCD}} a^e)^2 \tag{2.2}$$

and similarly for the heavy quarks. Here d_l vanishes as $(\mathcal{R}_l, \mathcal{R}_h) \to (\mathcal{R}'_l, \mathcal{R}'_h)$. Together with a similar demonstration that the difference between R_a/R'_a and unity can be neglected, this implies

$$\left(\frac{\tilde{Z}'_l}{\tilde{Z}_l} \right) = 1 + d_l \Lambda^2_{\mathrm{QCD}} \left(a(32^3)^2 - a(24^3)^2 \right). \tag{2.3}$$

For sufficiently close scaling trajectories, d_l is small and the $\mathcal{O}(a^2)$ term on the right can be dropped. This observation allows us to fix the relation between 24^3 and 32^3 quark masses and lattice spacings across the whole range of our data prior to performing the combined fit by using Z_l, Z_h and R_a determined above.

3. Combined fit strategy

We wish to perform a combined fit to both ensemble sets, using the values of Z_l, Z_h and R_a determined above to relate the quark masses between the lattices. The chiral/continuum fit forms are obtained by performing a double-expansion in the quark masses and lattice spacing about $a = 0$ and some general quark masses m^m_l and m^m_h. This gives forms which have the structure

$$A + Ba^2 + C_f(\tilde{m}_f - \tilde{m}^m_f) + D_f(\tilde{m}_f - \tilde{m}^m_f)a^2 + \dots, \tag{3.1}$$

where the index f is summed over l and h. We choose a power counting whereby terms of $\mathcal{O}(a^2 m)$ and higher are neglected.

We obtain chiral/continuum fit forms by extending the expansion to partially-quenched masses and take $\tilde{m}^m_l$ to be both the $SU(2)$ chiral limit and also some non-zero mass point. With the power counting defined above, the fit forms obtained by expanding about the chiral limit are the usual NLO partially-quenched ChPT fit forms with an additional a^2 coefficient. For example for the (unitary) pion decay constant we obtain the form

$$f_{ll} = f \left[1 + c_f a^2 \right] + f \cdot \left\{ \frac{8}{f^2} (2l_4 + l_5)\chi_l - \frac{\chi_l}{8\pi^2 f^2} \log \frac{\chi_l}{\Lambda^2_\chi} \right\}, \tag{3.2}$$

where $\chi_l = 2Bm_l$. We refer to these with the label 'ChPT'. We also include finite-volume corrections to the chiral logarithms in order to obtain a second ansatz which we label 'ChPTfv'. Finally, expanding about some unphysical quark mass and truncating at $\mathcal{O}(a^2 m)$ we obtain linear analytic
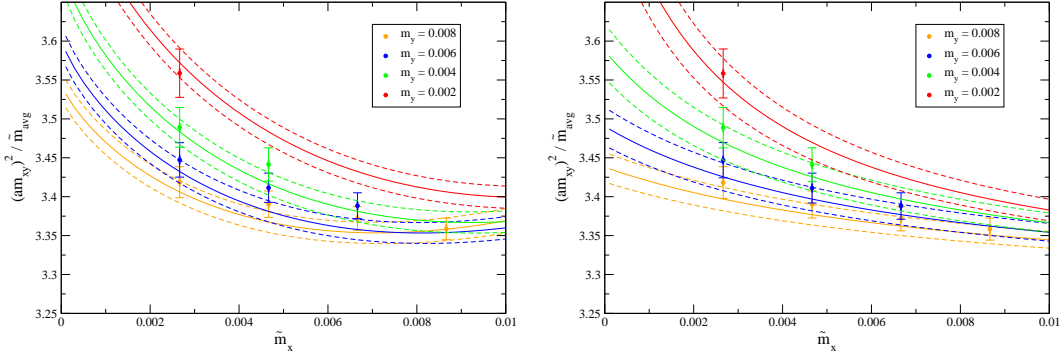
Figure 2: Plots of $2m_{xy}^2/(\tilde{m}_x + \tilde{m}_y)$ on the 32^3 $m_l = 0.004$ ensemble, overlaid by the ChPT (left) and analytic (right) fit curves. The data indicated by filled circular points was included in the fit and the heavier data points indicated by unfilled square points were not. The ChPT fit curves associated with the heavier masses above the cut do not well describe the data and cannot be seen within the plotted range.

fit forms (labelled 'analytic') of the form

$$f_{xy} = C_0^{f_\pi}[1 + C_f a^2] + \frac{1}{2}C_1^{f_\pi}(\tilde{m}_x + \tilde{m}_y) + C_2^{f_\pi}\tilde{m}_l. \tag{3.3}$$

The heavy quark dependence is always modeled as a linear expansion about the physical strange quark mass. Note that we do not expand around the SU(3) chiral limit as our previous analysis [3] showed that NLO SU(3) ChPT poorly described our 24^3 data.

In the matching analysis in the previous section we defined the quantities m_{ll}, m_{hl} and m_{hhh} to scale perfectly at a particular match point. Consider these quantities at quark masses $\tilde{m}$ (in physical units) away from the match point mass $\tilde{m}^{\text{match}}$. Setting the expansion mass of the double-expansion to $\tilde{m}^m = \tilde{m}^{\text{match}}$ we find that scaling imperfections arise as $a^2(\tilde{m} - \tilde{m}^{\text{match}})$, which is neglected by our power counting. As a result these quantities can be treated as artefact free and the a^2 dependence of their fit forms fixed to zero.

After performing a combined fit to the data, we match to the physical scaling trajectory by finding the values of m_l and m_h (in physical units) that give continuum values for m_π/m_Ω and m_K/m_Ω that are equal to their physical values, and the overall scale is set by fixing m_Ω to its physical value. This involves an elaborate iterative procedure which is described in detail in ref. [2].

In the remaining sections we discuss some of the results of our combined chiral/continuum analysis.

4. Evidence for chiral curvature

Figure 2 shows the ChPT and analytic fits overlaying the partially-quenched data on the lightest 32^3 ensemble. The values plotted are $2m_{xy}^2/(\tilde{m}_x + \tilde{m}_y)$, where the ratio is traditionally used to enhance the visibility of chiral curvature in the data. Both fit forms describe the data well within the range over which the fit was performed, but the ChPT form, unlike the analytic form, does not continue to describe the heavier data above the mass cut. The apparent curvature in the *linear* analytic fit forms is an artefact of the plot format, arising from the ratio of the data and the average valence quark mass; within our data we observe no statistically significant curvature.

Evidence for the existence of chiral curvature can be found by analysing the consistency of the analytic results with the predictions of Goldstone's theorem. The partially-quenched analytic fit form for the pion mass is

$$m_{xy}^2 = C_0^{m\pi} + \frac{1}{2}C_1^{m\pi}(\tilde{m}_x + \tilde{m}_y) + C_2^{m\pi}\tilde{m}_l. \tag{4.1}$$
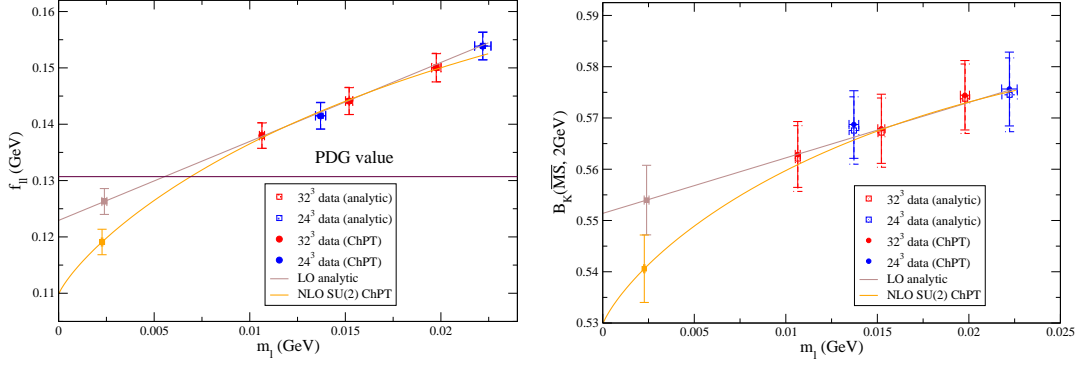
Figure 3: Comparisons of the chiral extrapolations of f_π (left) and B_K (right) using both the ChPT and analytic fit forms overlaying the data corrected to the continuum limit.

Goldstone's theorem states that the pion mass vanishes as the unitary light quark mass ($\tilde{m}_l = \tilde{m}_x = \tilde{m}_y$) goes to zero, which implies that $C_0^{m_\pi} = 0$. In practise we find that $C_0^{m_\pi} = -0.001(1)$, which is completely consistent. However, Goldstone's theorem also states that the pion mass should vanish in the limit of vanishing *valence* quark mass ($\tilde{m}_x = \tilde{m}_y = 0$), irrespective of the sea quark mass, and thus $C_2^{m_\pi} = 0$. We find $C_2^{m_\pi} = 0.43(8)$, which implies that chiral curvature must exist somewhere above the partially-quenched chiral limit. Of course this may happen at much lower pion masses than the physical mass, so we cannot rule out the validity of the analytic expansion for masses $m_\pi \geq 135$ MeV.

In figure 3 we show the chiral extrapolation of the pion decay constant in the continuum limit using both the ChPT and analytic fit forms. The analytic prediction for the physical f_π is 126(2) MeV, which is $\sim 3.4\%$ (2.2σ) lower than the PDG value of 130.4(2). We obtain an estimate of the finite volume corrections from the difference between the ChPTfv ($f_\pi = 121(2)$) and ChPT ($f_\pi = 119(2)$) results, giving 2 MeV. With this correction the analytic result is borderline consistent with the physical value. This implies only a small amount of chiral curvature can be exhibited in f_π above the physical pion mass. The NLO ChPT prediction for the physical f_π is however $\sim 9\%$ (5.7σ) too low, or 7.2% after finite-volume corrections are applied. This discrepancy is consistent with the expected $5\% - 15\%$ NNLO corrections, where these values are obtained by squaring the typical separation of our data from the LO decay constant f ($20\% - 40\%$). The evidence therefore suggests that the chiral behaviour of f_π is mostly linear in the region above the physical pion mass, and that higher order terms in the chiral expansion are required to describe this behaviour.

5. Physical predictions for the decay constants

Although the analytic formulae describe the data surprisingly well and appear to give a result for f_π that is more consistent with the physical value, there are strong theoretical arguments for chiral perturbation theory, and it may just be that higher order corrections are required to describe physics in the simulated mass range. We therefore choose to compromise between the two approaches by taking the central value as the average of the ChPTfv and analytic results, and include a chiral systematic error taken from the difference of these two results, thus covering both possibilities. We also include an additional systematic for the finite volume effects taken, as above, from the difference of the ChPTfv and ChPT results. In this scheme we find

$$f_\pi^{\text{continuum}} = 124(2)(5)\,\text{MeV} \tag{5.1}$$

$$f_K^{\text{continuum}} = 149(2)(4)\,\text{MeV} \tag{5.2}$$

$$(f_K/f_\pi)^{\text{continuum}} = 1.204(7)(25), \tag{5.3}$$

where the quoted errors are statistical and systematic respectively.

6. Physical predictions for the quark masses

The quark masses determined in the combined fits procedure are renormalised in a 'matching scheme' in which the renormalisation coefficient is unity on the 32^3 lattice and $Z_l(Z_h)$ for the light (heavy) quark. In this scheme we find

$$\tilde{m}_{ud} = 2.35(8)(9)\,\text{MeV} \qquad \text{and} \qquad \tilde{m}_s = 63.7(9)(1)\,\text{MeV}. \tag{6.1}$$

In order to convert these to the more conventional $\overline{\text{MS}}$-scheme, we first convert to an intermediate lattice scheme and then run to the conventional 2 GeV using the non-perturbative lattice data. The conversion to $\overline{\text{MS}}$ is then applied using perturbation theory at this higher scale.

The mass renormalisation factor in the lattice scheme is obtained from the renormalisation coefficient of the projected, amputated scalar bilinear vertex in several variants of the Rome-Southampton RI-MOM scheme [4]. In our previous analysis [5] we showed that a large systematic error arises due to the use of 'exceptional kinematics', where the incoming and outgoing momenta of the vertex are equal. This allows soft-momentum loops to occur even when the external momentum is large. The vertex therefore receives large contributions from momenta below the spontaneous chiral symmetry breaking scale, enhancing the effect of the breaking at these hard momenta. For this analysis we therefore use non-exceptional 'symmetric' momentum configurations, for which the incoming (p_1) and outgoing (p_2) momenta are different but obey the condition $p_1^2 = p_2^2 = (p_1 - p_2)^2 = q^2$. This allows us to assign an exact scale (q^2) to the vertex. We use two different symmetric-MOM (SMOM) schemes [6] defined using different projection operators. We also improve the determination of the renormalisation coefficients over the previous analysis by using volume source propagators to calculate the vertices. This leads to a very large reduction in the effects of gauge-field noise, vastly improving our statistical errors. The details of the determination of these renormalisation factors is discussed in greater detail in ref. [2]. Here we only quote the results in the $\overline{\text{MS}}$-scheme:

$$\tilde{m}_{ud}^{\overline{\text{MS}}}(2\,\text{GeV}) = 3.59(13)(16)\,\text{MeV} \qquad \text{and} \qquad \tilde{m}_s^{\overline{\text{MS}}}(2\,\text{GeV}) = 96.2(1.6)(2.1)\,\text{MeV}. \tag{6.2}$$

where the systematic (second) error includes the NPR error.

7. Physical predictions for B_K

Finally we obtain physical predictions for the neutral kaon mixing parameter B_K using our combined fitting procedure. B_K is defined as the non-perturbative contribution to $\bar{K}^0 \to K^0$ mixing. In combination with experimental results for the measure of indirect CP-violation ε and perturbation theory for the hard-scattering kernel, B_K can be used to measure the CKM matrix phase δ which parameterises all CP-violation in the Standard Model. It is calculated on the lattice using an effective four-quark operator

$$\mathscr{O}_{VV+AA} = (\bar{s}\gamma^\mu d)(\bar{s}\gamma^\mu d) + (\bar{s}\gamma^5\gamma^\mu d)(\bar{s}\gamma^5\gamma^\mu d). \tag{7.1}$$

normalised by the square of the $\langle 0|A_0|K^0\rangle$ matrix element:

$$B_K = \frac{\langle \bar{K}^0|\mathscr{O}_{VV+AA}|K^0\rangle}{\frac{8}{3}\langle K^0|A_0|0\rangle\langle 0|A_0|\bar{K}^0\rangle}. \tag{7.2}$$

As before we apply our chiral/continuum power counting to expansions about the chiral limit and a non-zero mass point, giving analytic, ChPT and ChPTfv fit forms. For example, the ChPT fit form is

$$B_K^{xh} = B_K^0\left[1 + c_a a^2 + \frac{c_0\chi_l}{f^2} + \frac{\chi_x c_1}{f^2} - \frac{\chi_l}{32\pi^2 f^2}\log\left(\frac{\chi_x}{\Lambda_\chi^2}\right)\right], \tag{7.3}$$

where h labels to the (fixed) strange quark, x labels the partially-quenched light valence quark, and $\chi_i = 2Bm_i$ as before. As B_K is a renormalisation scheme dependent quantity the fits must be performed to renormalised quantities. Here we use $\overline{\text{MS}}$ renormalisation coefficients calculated

via five intermediate non-perturbative lattice schemes: the RI-MOM scheme and four symmetric SMOM variants defined through the different choices for the projection operator of the four-quark vertex and of the pseudoscalar bilinear vertex with which it is normalised. For the final result we choose the lattice scheme for which the $\overline{\mathrm{MS}}$ conversion factors are best described by perturbation theory in the 2 GeV region at which results in this scheme are conventionally quoted. Here we present only the preliminary result of this analysis,

$$B_K(\overline{\mathrm{MS}}, 2\,\mathrm{GeV}) = 0.546(7)_{\mathrm{stat}}(16)_\chi(3)_{\mathrm{FV}}(14)_{\mathrm{NPR}}, \tag{7.4}$$

where the errors are the statistical error and the chiral, finite-volume and NPR systematics respectively. The chiral error is determined as before from the difference of the analytic and ChPTfv results. This difference is shown in figure 3, and is clearly much smaller than for f_π. More details of these calculations and an in-depth discussion of the other systematic effects can be found in ref. [7].

8. Conclusions

We have discussed and presented results from a simultaneous chiral/continuum extrapolation of two domain wall fermion ensemble sets. We described a procedure in which the lattices are matched first to an unphysical scaling trajectory running through the data, from which we obtain the relation between the quark masses and the ratio of cutoff scales between the lattices. We demonstrated that our data behave very linearly and that very little room is available for chiral curvature between our data and the physical point, certainly less than NLO ChPT suggests. However using Goldstone's theorem we showed evidence for the existence of chiral curvature on the pion mass in the partially-quenched direction. We discussed our strategy for estimating the systematic error on the chiral extrapolation and presented results for the decay constants, quark masses and B_K.

In future work we intend to include results from our new domain wall DSDR lattice action [8] which will enable us to simulate at significantly lower pion masses close to the physical point. Coupling this with our recent advances [9] in the non-perturbative renormalisation techniques will allow us to improve the systematic errors on all of the results presented in these proceedings.

The author would like to thank all members of the UKQCD and RBC collaboration.

References

[1] C. Kelly, P. A. Boyle and C. T. Sachrajda [RBC Collaboration and UKQCD Collaboration], PoS **LAT2009** (2009) 087 [arXiv:0911.1309 [hep-lat]].

[2] Y. Aoki *et al.* [RBC Collaboration and UKQCD Collaboration], arXiv:1011.0892 [hep-lat].

[3] C. Allton *et al.* [RBC Collaboration and UKQCD Collaboration], Phys. Rev. D **78**, 114509 (2008) [arXiv:0804.0473 [hep-lat]].

[4] G. Martinelli, C. Pittori, C. T. Sachrajda, M. Testa and A. Vladikas, Nucl. Phys. B **445**, 81 (1995) [arXiv:hep-lat/9411010].

[5] Y. Aoki *et al.*, Phys. Rev. D **78**, 054510 (2008) [arXiv:0712.1061 [hep-lat]].

[6] C. Sturm, Y. Aoki, N. H. Christ, T. Izubuchi, C. T. C. Sachrajda and A. Soni, Phys. Rev. D **80** (2009) 014501 [arXiv:0901.2599 [hep-ph]].

[7] Y. Aoki *et al.* [RBC Collaboration and UKQCD Collaboration], Provisionally entitled "Continuum Limit of B_K from 2+1 Flavor Domain Wall QCD" (2010)

[8] D. Renfrew, T. Blum, N. Christ, R. Mawhinney and P. Vranas, PoS **LATTICE2008** (2008) 048 [arXiv:0902.2587 [hep-lat]].

[9] R. Arthur and P. A. Boyle, [arXiv:1006.0422].